Imaging magmatic rocks on the Faroes Margin

A. W. ROBERTS,[1] R. S. WHITE,[1] Z. C. LUNNON,[1] P. A. F. CHRISTIE,[2]
R. SPITZER[1] and iSIMM TEAM[3]

[1] *Bullard Laboratories, Cambridge University, Madingley Road, Cambridge CB3 0EZ, UK (e-mail: rwhite@esc.cam.ac.uk)*
[2] *Schlumberger Cambridge Research, Cambridge CB3 0EL, UK*
[3] *iSIMM Team comprises N. J. Kusznir, R. S. White, A. M. Roberts, P. A. F. Christie, R. Spitzer, N. Hurst, Z. C. Lunnon, C. J. Parkin, A. W. Roberts, L. K. Smith, and V. Tymms*

Abstract: Break-up of the North Atlantic in the Paleocene was accompanied by widespread magmatism, which provides a challenge both to imaging basin structure and to modelling the subsidence and development of the continental margins. The rationale for new methods of seismic acquisition and modelling are reported here, followed by an illustration of the techniques with data from the Faroes region, which lay close to the hottest part of the mantle plume at the time of continental break-up. Igneous rocks were added to the crust during continental break-up on rifted margins as extrusive lavas, as sills intruded into the subsurface, and as lower crustal intrusions or underplate. Each provide different, but tractable problems to seismic imaging. It is shown that many of these difficulties can be surmounted by using very long offsets (long streamers or two-ship methods) with a broad-band, low-frequency source, and by using dense arrays of ocean bottom seismometers to provide complementary P- and S-wave velocity control. These methods are illustrated using new results from the integrated Seismic Imaging and Modelling of Margins (iSIMM) project, which acquired regional data across the Faroes shelf and margin in summer 2002. The iSIMM profile used 85 four-component ocean bottom seismometers and a 104 litre (6340 in^3) airgun array for wide-angle data, with vertical arrays for far-field source signature recording. The wide-angle profiles were overshot using three single-sensor, Q-Marine streamers, one 12 km long, the other two 4 km long. A 48-gun, 167 litre (10 170 in^3) deep-towed, broad-band airgun array was used with the Q-marine streamers. The airgun arrays were designed and tuned to enhance the bubble pulses, with peak frequencies at 8–11 Hz. They performed well, with excellent arrivals visible to ranges beyond 120 km on the OBS, and penetration through the basalts and well into the upper mantle. Examples are shown of the new seismic data, which enable imaging of the basalt flows and underlying sediments, as well as lower-crustal igneous intrusions. This allows good constraints to be placed on the igneous distribution and volumes on the rifted margin and adjacent continental shelf.

Keywords: rifting, magmatism, Faroe Islands, continent–ocean boundary, basalts, ocean bottom seismometers

There is an intimate link between rifting and magmatism along the continental margins of the northern North Atlantic. Along the 2500 km rift extending from northern Norway to the southern tip of Edoras Bank and along the conjugate coast of Greenland, massive intrusive and extrusive magmatism accompanied the continental break-up that occurred in the Palaeocene. The volcanic rocks, most of which are currently under water, total 1–2 million km^3, while the intrusives at or near the base of the crust bring the total igneous component added to the rifted margins to $8–10 \times 10^6$ km^3 (White & McKenzie 1989; Eldholm & Grue 1994). This massive outburst of igneous activity at the time of continental break-up exerts a number of important effects on the geology of the margins and their hinterland, many of which are particularly relevant to hydrocarbon exploration.

Influence of the Iceland plume

There is abundant evidence that the outburst of magmatism which accompanied the break-up of the North Atlantic was due to elevated mantle temperatures caused by the presence of the Iceland mantle plume (Fig. 1). The evidence is published in a number of papers: it includes the pattern of thickened crust on the margins and adjacent oceanic crust (White & McKenzie 1989; Barton & White 1997*b*); the rapidity of melt production, uplift and subsidence pattern on the margins (Bown & White 1995); the depth of melting inferred from rare-earth element inversions (White & McKenzie 1995); the geochemistry of the igneous rocks (Saunders *et al*. 1997); the seismic and gravity anomaly evidence for igneous underplating and lower crustal intrusion (Barton & White 1997*b*; Morgan *et al*. 1989; Korenaga *et al*. 2000; Holbrook *et al*. 2001); and the ocean-wide pattern of variations in crustal thickness from break-up to the present day (White 1997). The mantle temperature anomalies required are not large: the maximum temperature anomaly at the time of break-up was likely to be of the order of only 150 K, which is less than 10% of the normal mantle temperature of about 1600 K.

Three estimates of the extent of the thermal anomaly at the time of continental break-up are shown in Figure 1. The circle (solid line), is the original estimate published by White & McKenzie (1989), based primarily on the distribution of rift-related igneous rocks. The spoke-like pattern (dashed line), is a modification by Smallwood & White (2002), based on the observation that the thickness of the melt emplaced varies little with distance from the centre of the plume. This suggests that the mantle temperature varied little over that distance. There is evidence from numerical convection modelling that starting plumes may arise as sub-vertical sheets of hot mantle, which could give rise to the spoke-like pattern shown before collapsing to a more axisymmetric shape. The third suggestion (dotted elliptical line), by Jones & White (2003), is based on the distribution of igneous rocks and subsidence measurements. It shows the initial mantle thermal anomaly extending over a larger area than the other two: this is mainly because they ascribe thickened early Eocene oceanic crust between Rockall and Newfoundland, and thick Eocene (chron 24-13)

ROBERTS, A. W., WHITE, R. S., LUNNON, Z. C., CHRISTIE, P. A. F., SPITZER, R. & iSIMM TEAM 2005. Imaging magmatic rocks on the Faroes Margin. *In*: DORÉ, A. G. & VINING, B. A. (eds) *Petroleum Geology: North-West Europe and Global Perspectives—Proceedings of the 6th Petroleum Geology Conference*, 755–766.

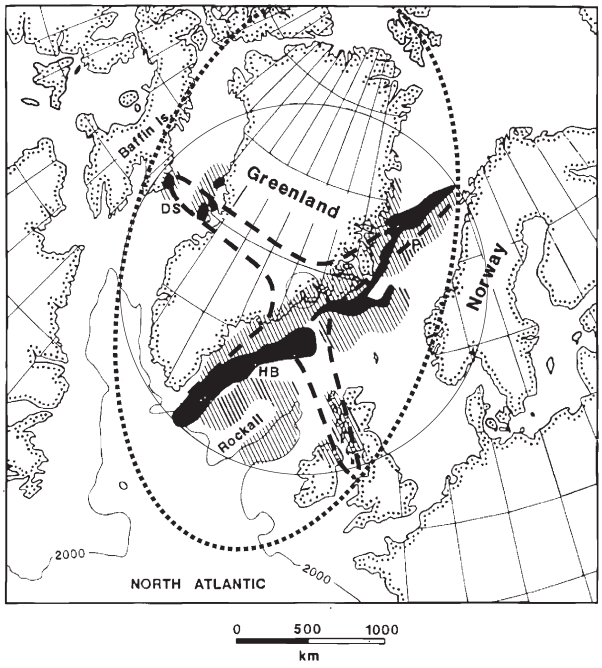

Fig. 1. Reconstruction of the northern North Atlantic at 55 Ma, shortly after the onset of seafloor spreading (after White & McKenzie 1989). Solid shaded area shows known extent of lava flows and hatched area shows extent of sills emplaced during continental break-up. Note that the extent of any igneous rock emplaced beneath mainland Greenland is unknown due to the ice cover, although an approximately east–west track of circular magnetic anomalies across central Greenland (Roest & Srivastava 1989; Brozena 1995) may represent a line of igneous centres. Three estimates of the extent of the mantle thermal anomaly at the time of break-up are marked: circular shape (solid line) from White & McKenzie (1989); spoke-like pattern (dashed lines) from Smallwood & White (2002) assuming rising sheets of asthenospheric mantle; elliptical shape (dotted line) from Jones & White (2003) also accounts for observed subsidence and ascribes thickened Eocene oceanic crust at the Gakkel Ridge and Newfoundland Sea to the same plume anomaly. The reconstruction uses an equal area Lambert stereographic projection.

oceanic crust formed at the Gakkel Ridge north of Greenland as being generated by the same thermal anomaly as created the rest of the igneous extrusions marked on Figure 1. However, the important conclusion for this study is that whichever map of the mantle thermal anomaly is used, the nascent Faroes Island region ('F' on Figure 1), lay close to the centre of the anomaly and therefore close to its hottest part and the greatest production of magma.

The present position of the mantle plume directly beneath the North Atlantic spreading centre provides a sensitive mantle thermometer, because oceanic crustal thicknesses are directly dependent on the mantle temperature (White *et al*. 1992). Prominent V-shaped ridges (Vogt 1971) observed on the Reykjanes Ridge in both the gravity and topography fields south of Iceland have been interpreted as caused by variations in crustal thickness and are consistent with the temperature of the mantle plume having varied by about 30 K on a 3–5 Ma timescale (White 1997; Smallwood & White 1998). Similar, but weaker gravity anomalies are present in the older parts of the oceanic crust adjacent to the continental margins. The crust in these regions is buried beneath sediments, which reduces the size of gravity anomalies (White 1997). Mantle plume temperature variations are crucial in assessing the hydrocarbon potential of the adjacent basins because they cause rapid regional uplift and subsidence, and have been postulated to control sedimentation pulses off the adjacent hinterland (White & Lovell 1997).

In this paper, seismic methods are discussed for imaging the igneous rocks on the Atlantic continental margin near the Faroe Islands, with examples to illustrate a variety of geological settings. Different techniques have to be employed to image extrusive lava flows, sills intruded into the sedimentary section, and lower-crustal underplating or intrusion. Yet all three igneous components have to be imaged well in order to build a full geological picture of the evolution of a volcanic rifted margin.

The data come from the region near the Faroe Islands, which was the most volcanically active portion of the North Atlantic margins in the early Cenozoic (Sorensen 2003). Extrusive lavas dated 61–55 Ma reach thicknesses of up to 7 km near the Faroe Islands, and are underlain by a thick underplated or igneous intruded lower crust (Richardson *et al*. 1998, 1999). Flood basalts created at the time of break-up between the Faroe Islands and east Greenland extend over 250 000 km^2 (Andersen 1988; Waagstein 1988; Larsen *et al*. 1999), at least 40 000 km^2 of which lie in the Faroe–Shetland Basin (Naylor *et al*. 1999). The lavas flowed ~150 km eastward away from the Faroe Islands, thinning out to zero in the Faroe–Shetland Trough (White *et al*. 2003). The total igneous component immediately after break-up reaches a thickness of 30–35 km on the adjacent Faroe–Iceland Ridge (Smallwood *et al*. 1999).

The iSIMM (integrated Seismic Imaging and Modelling of Margins) profiles (see also Smith *et al*. 2004), extend 120 km over the adjacent oceanic crust, in order to measure igneous crustal thickness variations following the first 15 Ma after break-up. The iSIMM project seeks to characterize magmatic ocean margins and to develop new models for their evolution by a combination of improved seismic acquisition and processing with better modelling of margin formation, including the effects of depth-dependent stretching, mantle plume temperature variations and igneous addition to the crust (White *et al*. 2002). This paper focuses on the 400 km long profile acquired by the iSIMM project Andersen 1988 over the Faroe margin with 85 ocean bottom seismometers (OBS) and three single-sensor streamers (Fig. 2). The OBS recorded data to offsets of more than 120 km, and the streamer to a maximum offset of 12 km.

Strategies and techniques for imaging through basalt

Basalt flows in sedimentary sections create a major impediment to seismic imaging of the underlying structure, particularly in the Faroes region where they are both pervasive and thick. Basaltic flow sequences typically consist of a multiple stack of individual flows that vary in thickness laterally; often with rugose tops and bases; frequently with strong physical property variations through the thickness of each flow resulting from changes in vesicle density, grain size and weathering; and in the case of the flows on the Faroes shelf, often with rubble or sedimentary horizons between individual flows, because they were deposited close to sea level. The net effect on a seismic signal traversing such a sequence is scattering, mode conversion between P- and S-waves, and interbed multiple generation. This tends to break up the coherence of transmitted signals, to act as a high-cut filter which only allows low frequency energy to be transmitted coherently, and to generate strong multiples that may mask weaker underlying reflections.

Apparent Quality factors (Q) in basalt sequences are generally low, leading to loss of high frequencies as energy propagates through them. In the Lopra 1/1A borehole, which penetrated some 3600 m of Lower Series basalt flows in the Faroes, Christie *et al.* (2002), estimated Q to be 35 from a vertical seismic profile (VSP). From a borehole through similar aged basalts in the north Rockall Trough, Maresh *et al*. (2003), found similarly low-Q values of 15–35 from spectral analysis of VSP data.

In general, conventional seismic reflection profiling images subhorizontal sedimentary reflections well, so the sediments overlying the basalt flows, and indeed the top of the basalts and sometimes the internal structure, are often resolved by conventional methods. Where the basalts are thin, again conventional near-vertical incidence seismic profiling techniques may work well in imaging the base of the flows and beneath. However, where the basalts

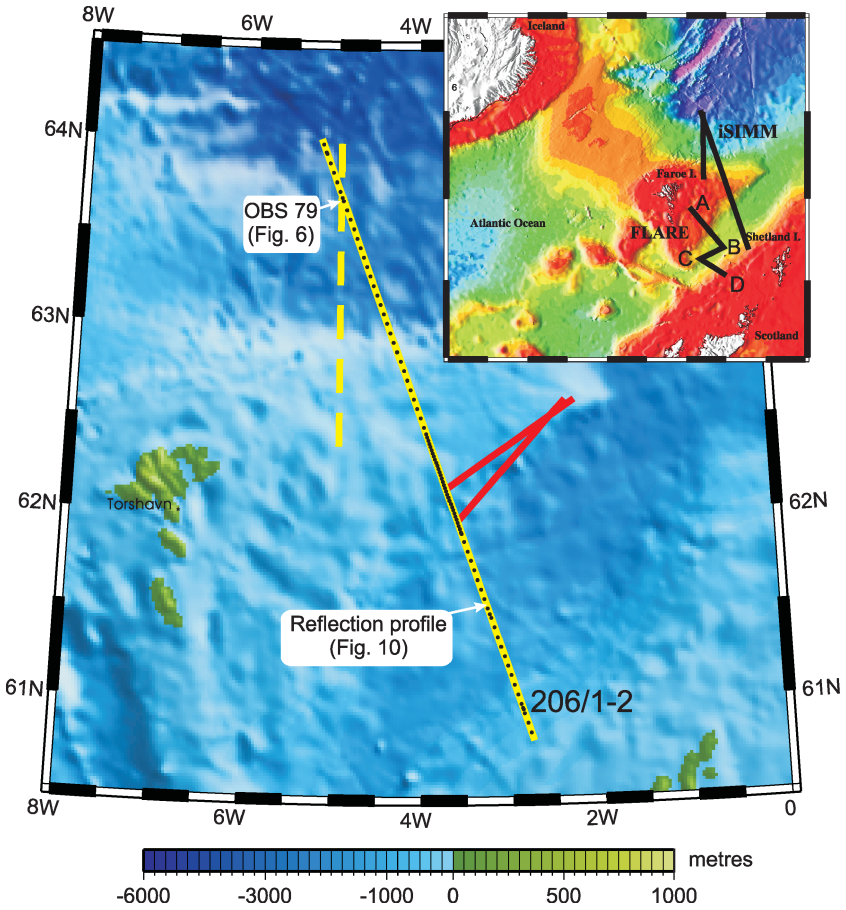

Fig. 2. Location map of the profiles shot across the Faroes margin. Black dots mark 85 OBS and three vertical array positions which were overshot by *RRS Discovery*. The same line was acquired by WesternGeco's *MV Geco Topaz* shooting into a multiple Q-streamer swath (solid yellow line). *Topaz* also acquired a second, north-south transect across the continent–ocean transition (broken yellow line), and *Discovery* also shot into the OBS along two offline tracks (red lines).

sequences are thick (several hundred metres or more), new techniques need to be employed. These fall into several categories, which are discussed below and illustrated with examples from the Faroes region.

One way to improve sub-basalt images is to tailor the seismic source signal to the transmission properties of the basalt. This means producing more energy at low frequencies. Secondly, the low-frequency response of the streamer is most readily enhanced by towing at a greater depth than is normal, as the deeper the tow, the lower is the dominant frequency enhanced by the ghost operator. A deeper tow also improves the characteristic of the low frequency roll-off into the DC response. It should be noted that the number of octaves over which the ghost operator enhances the signal remains constant at 2.32, whatever the tow depth. The third improvement that can be made to conventional (6000 m offset) streamer data is to tailor processing of the seismic data to the sub-basalt target, including taking care over shot-by-shot signature deconvolution, and pre-stack depth migration using appropriate velocity fields. These three improvements can all be applied to conventional source and receiver geometries and are capable of delivering significant improvements to the sub-basalt images.

Conventional seismic reflection profiling focuses exclusively on the sub-critical part of the waveform, and usually any arrivals outside the water-wave cone (including refractions or diving waves and wide-angle reflections) are muted before processing. However, the wide-angle arrivals carry considerable information about the subsurface and indeed the wide-angle reflections generally have higher amplitudes than the shorter-offset reflections, because the amplitude of a reflection increases as the critical angle is approached. So the fourth approach to improving sub-basalt imaging is to record data to longer offsets than normal and to use the wide-angle arrivals to image the deep structure.

Seismic acquisition

Low frequencies allow penetration through basalts. For example, low-frequency (5–20 Hz) data have enabled imaging of the Corrib gas field reservoir beneath shallow basalts offshore Ireland (Dancer *et al*. 2004). Ziolkowski *et al*. (2003) reported improved penetration through basalts on the Faroes shelf by towing large guns at 15 m depth. Large airgun arrays towed deep can produce strong low-frequency signals capable of propagating hundreds of kilometres through igneous rocks. For example, on the Faroe–Iceland Ridge a 153 litre (9324 in^3) airgun array towed at 10 m depth produced good seismic arrivals to ranges beyond 400 km along the Faroe–Iceland Ridge (Staples *et al*. 1999).

Gun depth. One of the simplest ways to control the dominant frequency of an airgun is to vary its depth. By taking advantage of the phase reversal of reflections from the sea surface, it is possible to enhance the downgoing energy by choosing a depth such that the sea-surface reflected ghost interferes constructively with the primary downgoing wave: for a vertically downward travelling wave, constructive interference occurs at a wavelength four times the depth.

For the iSIMM profiles, an airgun array including guns as large as 16 litre (1000 in^3) were towed at 18–20 m depth to produce energy below 10 Hz, and to give good output up to 20 Hz, and used a range of gun sizes to produce as flat a spectrum as possible, as

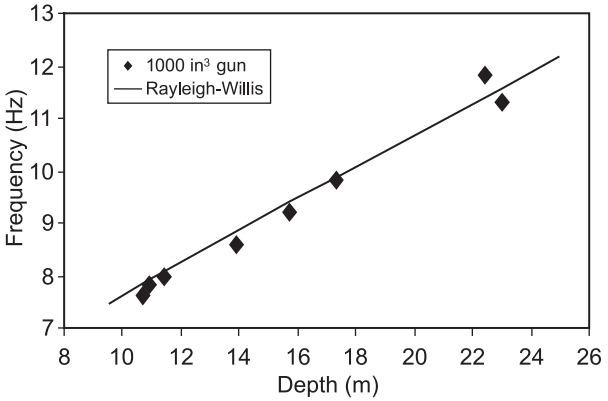

Fig. 3. Measured bubble frequency versus depth, estimated from a hydrophone located 1 m from a single 16.4 litre (1000 in^3) gun test-fired during the Faroes iSIMM survey. Over the 11–23 m depth interval, the trend follows the Rayleigh–Willis prediction, of increasing frequency with increasing depth. The frequency was measured by picking the second and third peaks from the recorded gun signature. The first peak was not used, as this is the initial out-rush of air, and is not representative of the frequency of the ensuing oscillations.

described in the next section. A plot of the measured bubble oscillation frequency from the 1000 in^3 gun is shown in Figure 3. Note the similarity of the trend to the Rayleigh–Willis prediction.

Gun tuning. Sources were designed using large, deep-towed guns for the Faroes profiles, and explored the relative benefits of two tuning methods: synchronizing the guns to time-align the primary pulses (peak tuning); and introducing delays to time-align the first bubble (bubble tuning). Conventional peak tuning synchronizes the guns so that the first pressure peaks coincide (Fig. 4a). With bubble tuning (Avedik *et al*. 1996), firing delays are applied so that the first bubble oscillations coincide (Fig. 4b).

The Faroes OBS profile was shot twice, using a 14-gun, 104 litre (6340 in^3) array towed at 20 m depth, first with peak tuning and then with bubble tuning. The far-field waveforms were recorded with several deep-water vertical arrays of hydrophones. The unfiltered outgoing source waveforms from the peak and bubble tuning are shown in Figures 5a and b respectively. After filtering with a 20 Hz high-cut filter (Figs 5c and d), to represent the effect of the earth filter on the seismic waveform, it is clear that the

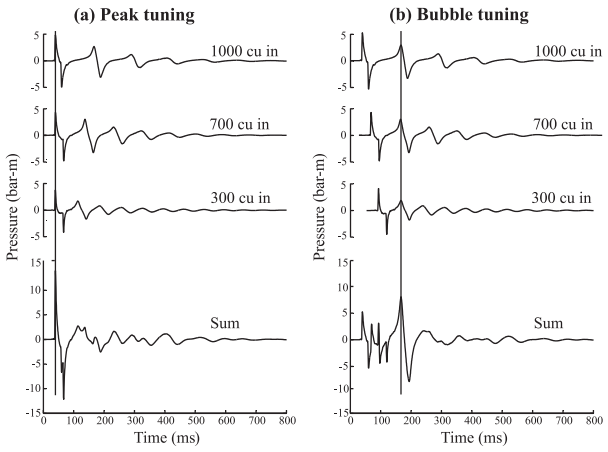

Fig. 4. Illustrative diagram showing superposition of three far-field single airgun signatures towed at 20 m depth to achieve (**a**) a source tuned on the peak to enhance the high frequency primary pulse, or (**b**) tuned on the bubble to enhance the lower frequency bubble pulse. The latter has a richer low frequency bandwidth at the cost of a complex front end. Each trace lasts 900 ms.

bubble-tuned waveform (Fig. 5d) has a higher ratio between the primary (largest) and secondary peak than does the peak-tuned waveform (2.0 compared to 1.8), and has a markedly shorter coda than does the peak-tuned signal (Fig. 5c). Both these characteristics are desirable for identifying and modelling arrivals on very long-offset data, and mean that the bubble-tuned data is superior for deep crustal imaging. A comparison of very long-offset OBS data from peak and bubble tuning recordings bears out this conclusion (Fig. 6): on the iSIMM Faroes project we have recorded multiple OBS data out to offsets of 140 km, which will provide good control on the lower crustal and upper mantle structure (Lunnon *et al*. 2003).

For the 12 000 m Q-streamer profiles, we designed a bubble-tuned source on similar lines, producing a 48-gun, 167 litre (10 170 in^3) array towed at 18 m depth with peak output at frequencies of 9–11 Hz. For this source we were able to monitor the shot-by-shot waveform using calibrated near-gun hydrophones from which the far-field waveform could be computed using the notional source algorithm of Ziolkowski *et al*. (1982). This allows shot-by-shot designature, which is important prior to processing because the bubble-tuned source array produces a complex waveform, particularly at the front end (e.g. Fig. 5a).

Seismic receivers: use long offsets. Long-offset arrivals carry considerable information on the lower crust, both in the form of wide-angle reflections (which attain high amplitudes near their critical angle), and diving waves. There are three main techniques for recording very long-offset data. The first is to use two ships and multiple passes along the profile. This has been used successfully on the Faroes shelf to achieve offsets of over 38 000 m from three passes of two ships along the profile at different separations (e.g. White *et al*. 1999). In principle, any arbitrary maximum offset can be achieved by multiple passes of two seismic ships at increasing separations. There are various drawbacks of this method. First, the flip-flop shooting means that the fold of coverage is halved compared to single ship firing into a single streamer. Second, the fact that two different sources and streamers must be used is in itself a disadvantage, and however much care is used in matching the sources and receivers, in practice there will always be some differences which will cause the waveform to vary with offset. Lastly, because each streamer is liable to feather independently, the assumption of locally 2D structure (i.e. that the structure is invariant perpendicular to the profile) has to be made in the processing.

The second and obvious method of attaining larger offsets is to increase the length of the streamers: at present, 12 000 m streamers are available for 2D surveys. In the iSIMM survey three streamers were deployed, with a 12 000 m streamer in the centre, and two 4000 m streamers towed at 150 m to either side. This gives a measure of 3D control, particularly on the shallow subsurface structure and on returns scattered from rough surfaces. Relative positioning between the streamers was recorded by acoustic cross-bracing, which allows the three hydrophone streamers to be used to estimate directions of wavefronts moving across the streamer antennae. Extremely good velocity control in the upper crust is available from the moveout of the long-offset data (Fig. 7).

The third way to record to larger offsets is to use fixed seafloor receivers, either in the form of seafloor cables or of autonomous ocean bottom seismometers. This then allows any offset to be recorded, simply by steaming the shooting ship further away. Along the iSIMM profile shown here, good wide-angle seismic arrivals were recorded by OBS from the entire crust and into the upper mantle (e.g. Fig. 6). There is a further considerable advantage of seafloor receivers, which is that three-component seismometers may be deployed in addition to hydrophones. This enables the direct recording of shear waves, the separation of upgoing and downgoing wavefields (useful for water multiple suppression), and direct measurement of particle motions which may help invert for anisotropy in the subsurface. The disadvantage

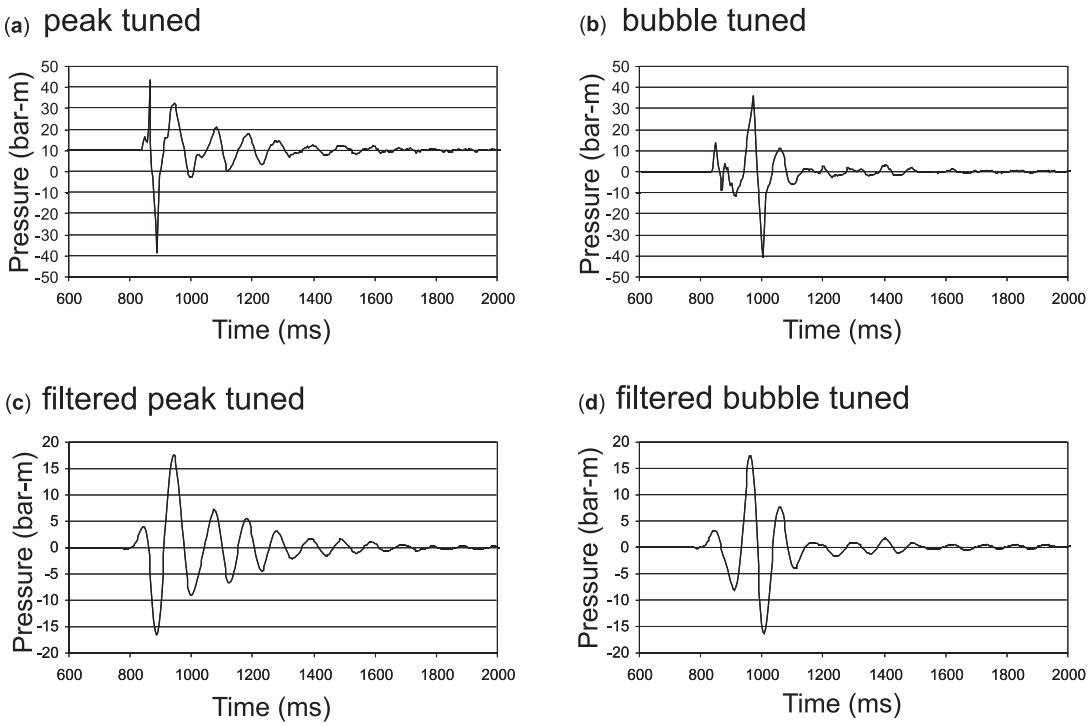

Fig. 5. Far-field signature of OBS sources: (**a**) peak tuned; (**b**) bubble tuned; (**c**) peak tuned after 20 Hz low-pass filter; (**d**) bubble tuned after 20 Hz low-pass filter. Note the more compact (with fewer reverberations) bubble tuned signature in (d).

of this method of recording data is the spatial inflexibility and sparsity, and extra cost of fixed seafloor receivers. In the iSIMM project the advantages of the latter two methods were optimized by recording long-offset streamer data with its high spatial sampling in addition to fixed OBS data that give better control on the deep structure and on converted waves.

Seismic processing: old and new methods. Without going into detail about seismic processing methods, it is worth highlighting some areas where improvements are being made, and are likely to progress further. The increased power of computers means that the ability to process large amounts of data is improving continuously, and it is routinely shown that significant improvements are often achieved simply by re-processing the same seismic data a few years later, after processing power and algorithms have improved. With careful attention to tailoring the processing to the problem in hand (such as emphasizing the low-frequency bandwidth for sub-basalt imaging), it is already easier to achieve sub-basalt images than it was a decade ago, especially where the basalts are relatively thin. A notable new technique that can markedly improve the final image is to record the signature of the airgun source on a shot-by-shot basis, as was done on the iSIMM profiles, which then allows predictive shot designature, rather than having to rely on conventional statistical shot deconvolution methods.

In the context of imaging beneath thick basalt flows, a major problem is the abundance of intra-bed and inter-bed multiples and of mode-converted energy that arises because there are such strong contrasts in physical properties between the basalt and sediment layers. This means that although there may be many strong reflectors in the subsurface, it is often impossible to know which of them are primary reflections, and therefore what they represent. The acquisition of long-offset profiles helps with this problem by providing the opportunity to get much better deep velocity control (Figs 6 and 7), which improves pre-stack migration imaging and discrimination against multiples.

Another way in which long-offset profiles can assist is to enable the separation of high-amplitude, first arriving wide-angle reflections of known origin beyond the water wave cone, and to migrate those back to normal incidence (White *et al*. 2003). A good example is the base-basalt reflection, which forms a strong wide-angle reflection on seismic data recorded on the Faroes shelf (Fliedner & White 2001). Using a velocity model of the subsurface derived from tomographic analysis of the wide-angle arrivals, the base-basalt reflection can be migrated back to normal incidence and superimposed on the pre-stack depth migration (PSDM) of the same profile derived from the conventional short-offset data (Fig. 8). Although the migrated wide-angle reflection is of low frequency, and therefore has relatively poor resolution, it enables the unambiguous identification of which of the many reflections (including many multiples) on the higher-resolution conventional PSDM profile is the real base-basalt reflection, which is a great asset in interpretation. Similar analyses can be made to identify other deep reflections, such as the Moho reflection discussed below, which can be seen where the iSIMM profile crosses the continent–ocean boundary.

The combination of long-offset streamer data and closely spaced long offset OBS profiles on the iSIMM line enables good velocity models to be derived from the OBS data, and then the image on the streamer data to be improved by applying these velocity models to the stacking and migration steps. The ability directly to detect shear waves on the OBS using the three-component seismometers also enables identification of which wide-angle arrivals on the streamer data are converted shear waves, to determine the S-wave velocity structure, and then to use the much denser streamer data to form independent converted S-wave images of the subsurface structure. That there is strong doubly converted shear wave energy on streamer data in this region is shown by the shot gathers from the FLARE data illustrated in Figure 9. The ability to measure both compressional and shear wave velocities using the OBS also provides opportunities to characterize the composition and petrology of subsurface material, and is useful in discriminating between ‘hard’ (igneous sill) and ‘soft’ (sedimentary layer) causes of high-amplitude reflectors. Finally, as well as the possibility of AVO analysis the recording of seismic arrivals to larger offsets, together with the measurement of particle motions on bottom seismometers, provides opportunities to investigate the velocity anisotropy of subsurface rocks: since anisotropy can

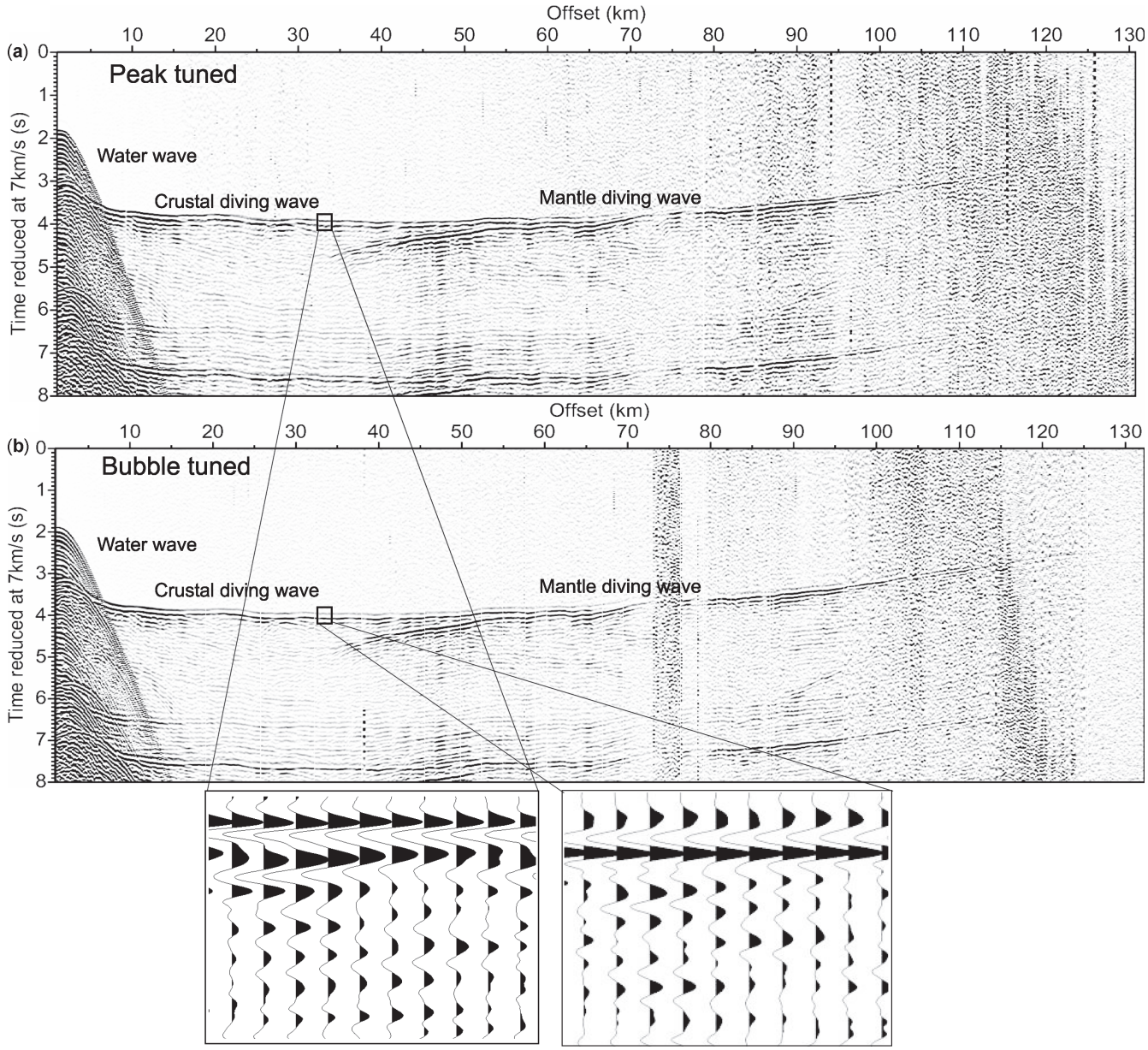

Fig. 6. OBS 79 (see Fig. 2 for location) receiver gathers: (**a**) peak tuned; (**b**) bubble tuned. Note the sharp wide-angle Moho reflection, which attains high amplitude beyond 35 km offset as the critical distance is approached. Data is band-pass filtered 3–18 Hz, and only every second trace is displayed after a running trace mix. Reduction velocity of 7 km/s means that arrivals with a phase velocity of 7 km/s are horizontal in this display. Enlargements show the more compact nature of the bubble-tuned source.

reach 20% between vertical and horizontal in sediments, this is crucial for stacking, for imaging and for depth-conversion of seismic data.

Imaging magmatic rocks in the Faroes Region

Figure 10 shows examples of imaging extrusive and intrusive basalts from a 400 km long seismic profile, extending from the edge of the continental Shetland platform in the southeast to the Cenozoic oceanic crust of the Norwegian Sea in the northwest. The profile traverses several distinct provinces, including the stretched continental crust of the Mesozoic Faroe–Shetland Trough, the shallow Fugloy Ridge in the central part of the profile, where basalt flows lie just beneath the seafloor, the volcanic continent–ocean boundary generated by early Cenozoic continental break-up and fully oceanic crust in the northwest. There are few wells in this region, but the profile crosses one deep well (206/1-2), which provides stratigraphic control in the Faroe–Shetland Trough down to the Maastrichtian (Fig. 10). The OBS were spaced at 6 km intervals, except for near the well and across the subsurface basalt escarpment, where they were more closely spaced at 2 km intervals to provide better resolution.

In the Faroe–Shetland Trough, large tilted fault blocks are visible in the basement and extensive igneous sills intrude the sediments. The typically saucer-shaped sills in the Faroes–Shetland region have been imaged well by 3D seismic surveys (e.g. Smallwood & Maresh 2002), and will not be discussed further here. Two 25 km long extracts of this long regional profile are discussed below in more detail since they exemplify the different nature of the extrusive volcanism on the continent–ocean margin and on the continental hinterland. The extract across the continent–ocean boundary also demonstrates the seismic response of the lower crustal intrusions and the Moho on the margin.

The Faroes continent–ocean boundary

The most prominent feature of the volcanic rocks on the margin are the beautiful convex-upward seaward dipping reflectors

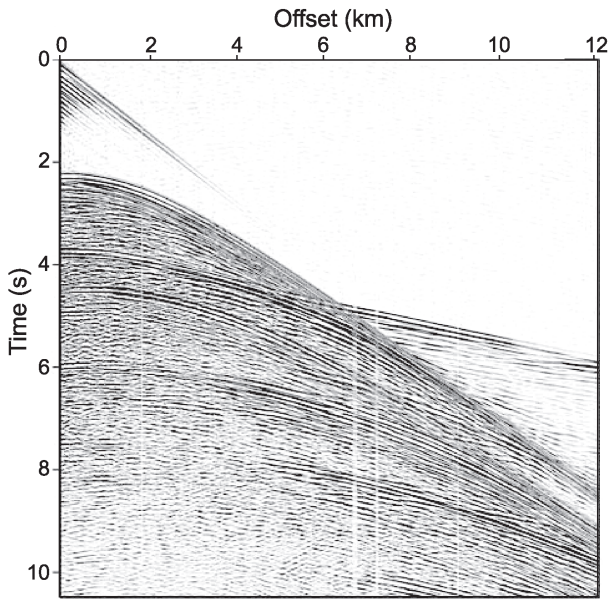

Fig. 7. Shot-gather from a single shot above the seaward dipping reflector sequence on the continental margin recorded by the 12000 m Q-streamer, after digitally group-forming individual sensor data into 12.5 m groups and shot designature.

(SDRs) illustrated in Figure 10. Individual reflectors are coherent over lateral distances of 20 km or more, and the entire package of SDRs attains a maximum thickness of 4 km adjacent to the oldest oceanic crust, thickening rapidly from the continental (south-eastern) to the oceanic (northwestern) part of the margin shown in Figure 11. The long lateral continuity of individual reflectors in the SDRs suggests that the lavas were flowing across a flat surface with little topography to impede or channel the flow. The SDRs that are imaged so well here probably do not represent the earliest stages of continental break-up: that may have been characterized by formation of rift blocks and graben, and the earliest flows would have had to fill in the pre-existing topography (e.g. Edoras Bank, Barton & White 1997*a*). However, by the time this effusive volcanism was extruded, it is apparent that little major faulting was occurring, and the margin was subsiding rapidly in a steady fashion to produce the arcuate shape of the lavas.

It is probable that the crust in the transition region between continent and ocean was so heavily intruded that by the time the SDRs were being formed it had become hot and ductile, and responded to the ongoing stretching by ductile thinning. The transition region is very narrow (only a few tens of kilometres wide), which is in marked contrast to non-volcanic margins, where the continental stretching can extend over 250 km width: again this is probably due to the extensive igneous intrusion in this region which so weakened the crust that it focused further stretching into this narrow, weak region.

The lower part of the continental crust below the SDRs is marked by extensive, strong sub-horizontal reflectivity (Fig. 11a), with a seismically transparent region between the bottom of the SDRs and the top of the lower-crustal layering. This section is depth-converted in Figure 11b, using the high-resolution velocities derived from streamer semblance analysis of every gather for the sediments above the basalts, and the crustal velocities from wide-angle OBS arrivals for the deeper section. The depth-converted section emphasizes the considerable portion (15 km thick, more than half the total thickness) of the continental crust below the SDRs which exhibits strong layering.

The region of the lower crust with strong layering coincides with abnormally high seismic velocities above 7.2 km/s found from the wide-angle OBS analysis. These velocities are markedly higher than the seismic velocities found in the equivalent portion of lower crust under the adjacent British mainland, and are interpreted as due to the intrusion of mantle-derived magmas during continental break-up (White & McKenzie 1989). The primitive, iron and magnesium rich picritic lavas intruded in the lower crust are likely to have differentiated to produce the less dense, and so more buoyant tholeiitic lavas that were extruded to form the SDRs, leaving behind the denser (and higher seismic velocity) residual in the lower crust. Petrological models (Cox *et al.* 1980) suggest that the volume of residual melt left in the lower crust is likely to be two or three times the extruded volume, which is consistent with the relative thicknesses of

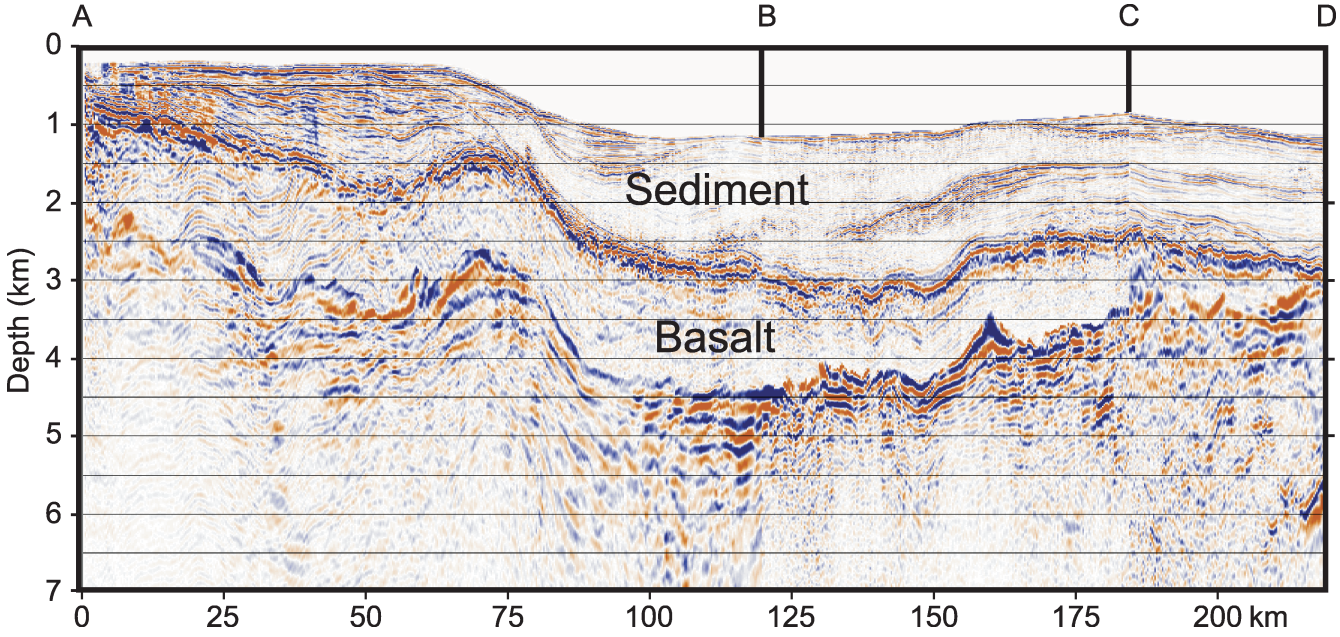

Fig. 8. Unfolded migrated seismic section (from White *et al.* 2003), highlighting the top (from conventional seismic processing) and base (from wide-angle reflections outside the water wave cone) of the basalt flows from FLARE lines extending from thick basalts near the Faroe Islands to the feather edge of the sub-surface basalt flows beneath the Faroe–Shetland Trough (see Fig. 2 inset for location). Location of points A–D are marked on Figure 2.

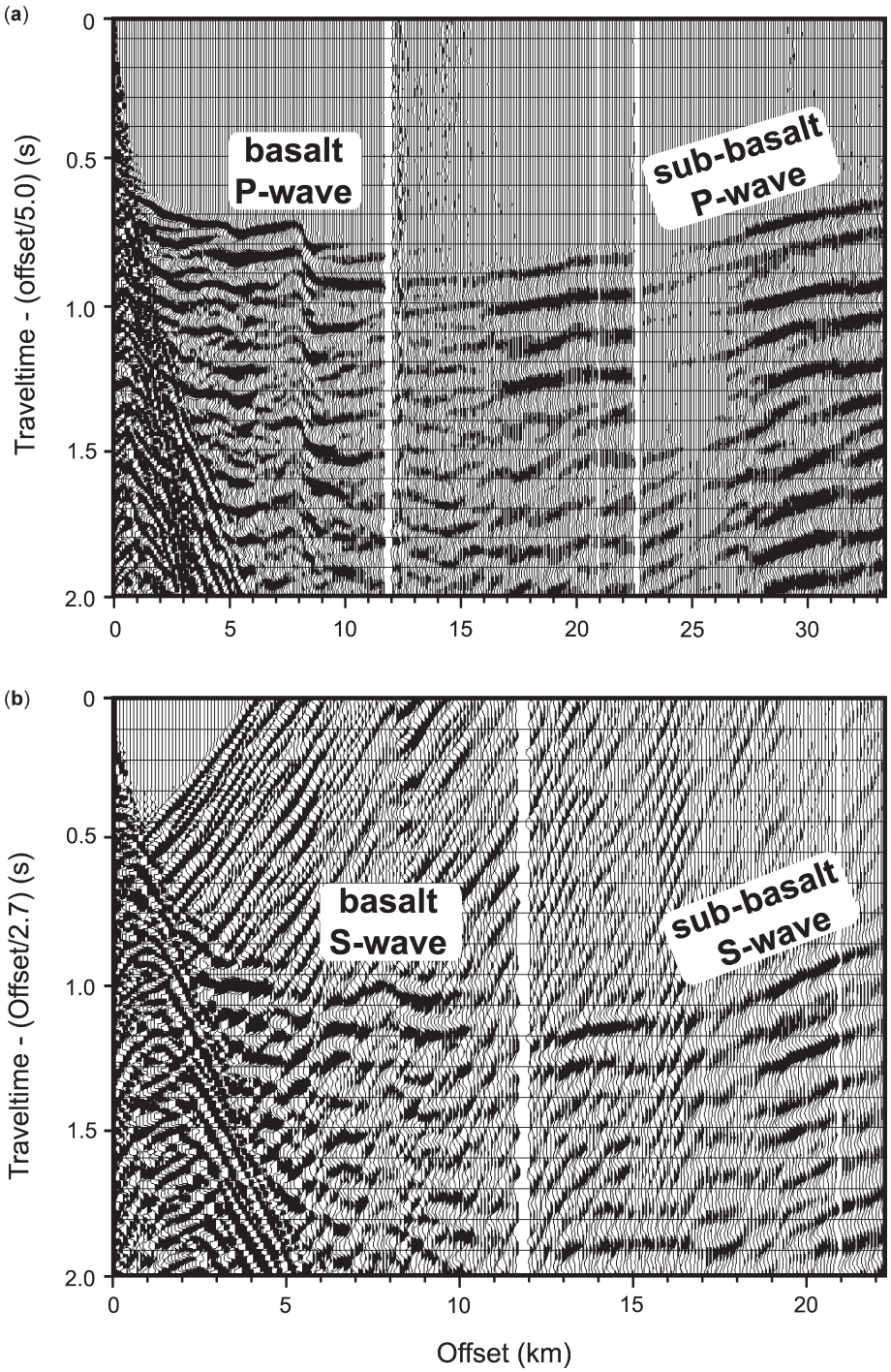

Fig. 9. Example of a single shot supergather from two-ship profile shown in Figure 8, with the shot-point at 0 km along the profile and offsets increasing southeastward. The 2D structure along the profile causes irregularities in the arrivals; the data gaps at ~12 km and ~23 km are a consequence of the construction of supergathers using two ships with flip-flop shooting (see White *et al.* 1999 for details). (**a**) Shot gathers reduced at 5 km/s to highlight the P-wave arrivals from the basalt and sub-basalt layers; (**b**) the same shot gather reduced at 2.7 km/s to highlight the doubly converted S-wave arrivals from the same layers.

Fig. 11. Section of seismic profile crossing the seaward dipping reflector sequence on the continent–ocean boundary (see Fig. 10 for location of this 25 km long extract). Processing includes source designature, multiple suppression and migration. Note the superbly imaged SDRs, interpreted as lava flows extruded near sea level from the developing Atlantic rift and flowing landward over the hinterland; the strong lower-crustal layering coincident with high-velocities, presumed to represent lower-crustal intrusions; and the sharp Moho reflection which thins markedly from continental (southeast) to oceanic (northwest) crust. (**a**) Seismic data plotted in two-way travel time; (**b**) seismic data after depth conversion using sediment velocities from detailed semblance analysis of the streamer data and deeper crustal velocities from analysis of long-offset OBS data. A cross section of the velocity model used for the depth conversion is shown at the side of (b). It is taken at 140 km along the line. Reflection data shown with permission of WesternGeco.

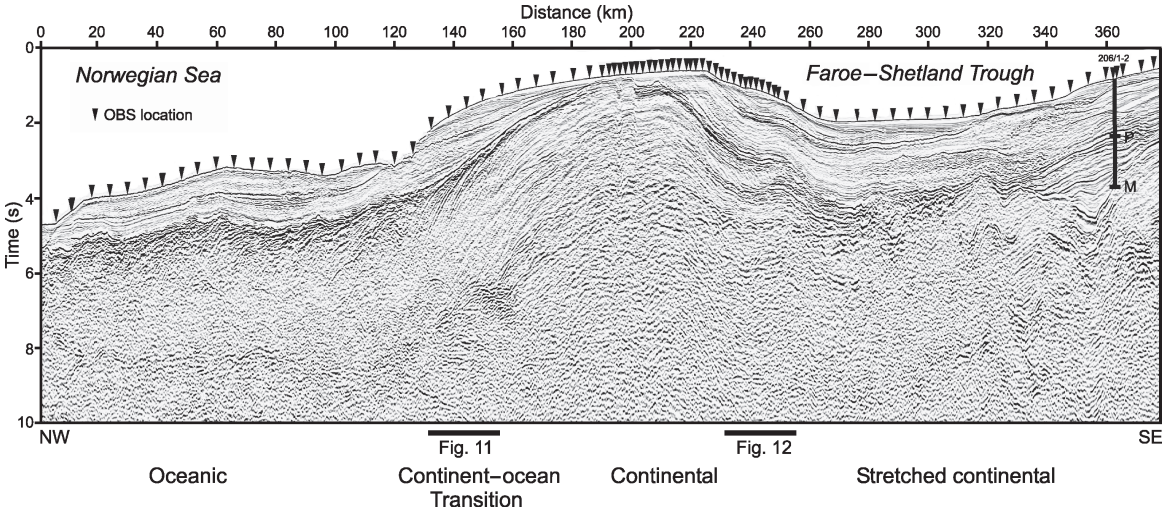

Fig. 10. Squash-plot of entire 375 km long Q-profile (see Fig. 2 for location), after source designature and multiple suppression, showing location of hole 206/1-2, which terminates in the Maastrichtian, and of OBS (triangles). P and M mark the tops of the Palaeocene and Maastrichtian layers. The positions of Figures 11 and 12 are also indicated. Data are shown with permission of WesternGeco.

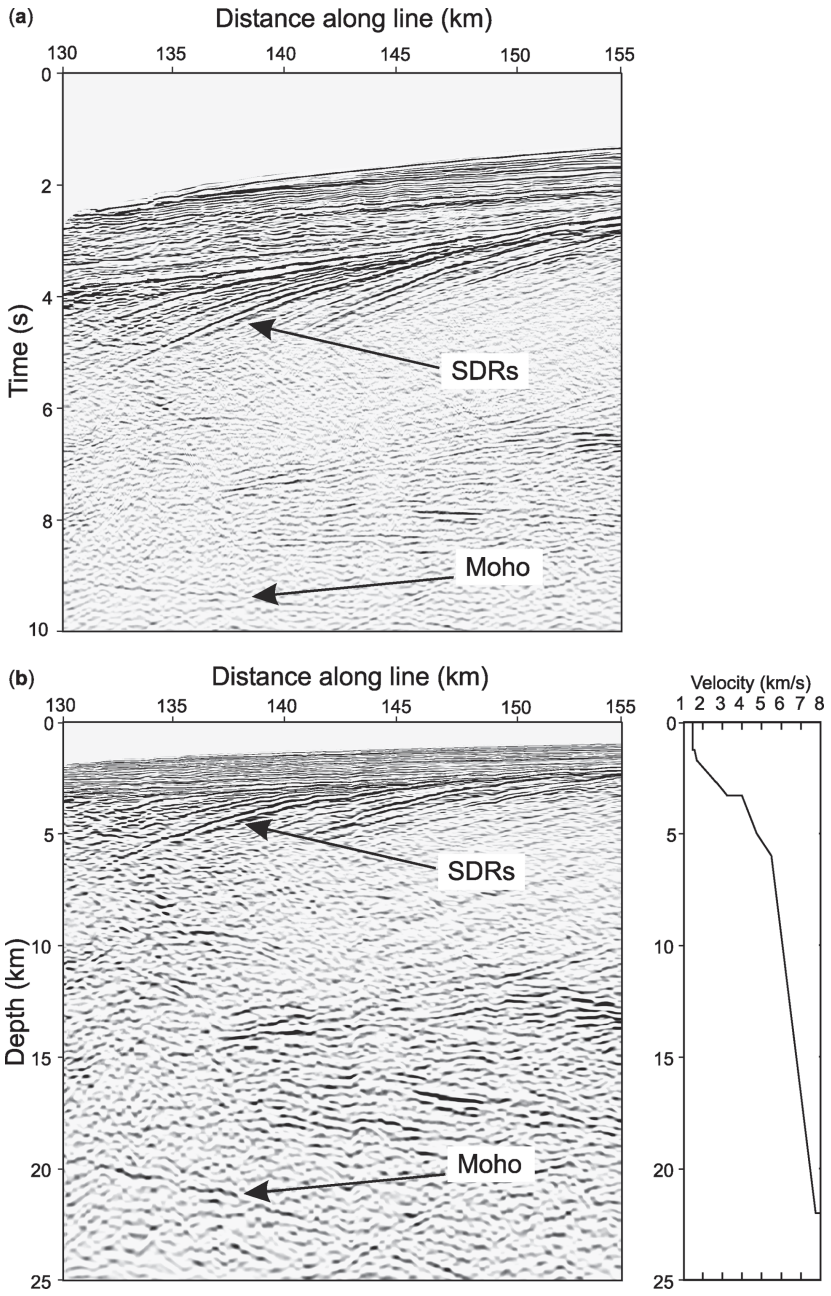

lower crust intrusions and extruded SDRs that we see on this margin. The lower crustal layering decreases greatly in intensity in the adjacent oceanic crust to the northwest. This is consistent with the decrease in contrast between physical properties that we expect in oceanic crust, where new melt is intruding a mafic crust of similar composition. By contrast, where mafic melts intrude continental crust, there may be a much larger difference in physical properties between the new melts and the pre-existing crust, which produces much stronger reflectivity.

Finally, the reader's attention is drawn to the strong, well-defined reflector at the base of the crust which shallows steeply from the continental to the oceanic crust (Fig. 11). This reflector is interpreted as marking the Moho discontinuity, based on the strong wide-angle reflections it produces on the OBS (Fig. 6), and the velocities derived from analysis of the OBS arrivals. Over a lateral distance of 15 km, the crust (excluding the post-basalt sediments) thins by one third, decreasing to 15 km thick under the oldest oceanic crust shown on Figure 11. This inferred Moho reflection lies beneath the lower continental crustal layering: the lower crustal layering and Moho were probably formed contemporaneously but, in the absence of any cross-cutting relationships or truncations, this hypothesis is uncertain. What is remarkable, however, is the abrupt nature of the reflector, which therefore marks a sharp boundary between the crust and the underlying mantle. The 15 km thick oceanic crust is considerably thicker than the crust formed above normal oceanic spreading centres away from mantle plumes, but it is consistent with the thickness of the oldest oceanic crust elsewhere on the northern North Atlantic margins (e.g. Barton & White 1997*b*; Korenaga *et al*. 2000; Holbrook *et al*. 2001), and is indicative of raised mantle temperatures caused by the plume.

The Faroes Shelf

The style of extrusive Paleocene volcanic rocks that flowed toward the continental hinterland (which experienced none or only a minor amount of stretching during the Cenozoic continental break-up), is quite different from that found on the rifted margin. Figure 12 shows a 25 km length extract from our regional iSIMM seismic profile to illustrate this. The lavas, produced in the volcanically active Atlantic rift to the northwest of this location, flowed up to 150 km landward across a pre-existing and partly sediment-filled landscape toward the Faroe–Shetland Trough, thinning as they flowed (White *et al*. 2003). Where they reached the palaeo-shoreline, they produced strong, southeastward dipping, sigmoidal reflectors within the basalt sequence. The sigmoidal reflections move upward and southeastward across the section as the lavas progressively built outward, pushing the coastline eastward (Kjørboe 1999). Strong sub-horizontal layering below the sigmoidal reflectors probably represents early hyaloclastites and lava flows from the first phase of volcanic activity in the Faroes region, while the equally strong layering above the top of the sigmoidal reflectors is probably caused by late lava flows crossing the entire region, capped by the ubiquitous Balder Ash layers.

Detailed velocity analyses play an important part in the interpretation. The Balder Ash which overlies the basalt flows is dominantly a sedimentary deposit, and exhibits a strong velocity gradient from typical unconsolidated sediment at the top to weathered basalt at the base. Beneath the bottom of the basalt sequence, velocity inversions inferred from the long-offset wide-angle data show the presence of sediments over which the early basalts flowed. Although their age is unknown, since they have not yet been drilled, the regional geology suggests that they are probably mainly Paleocene, lying above a rifted late Cretaceous basement.

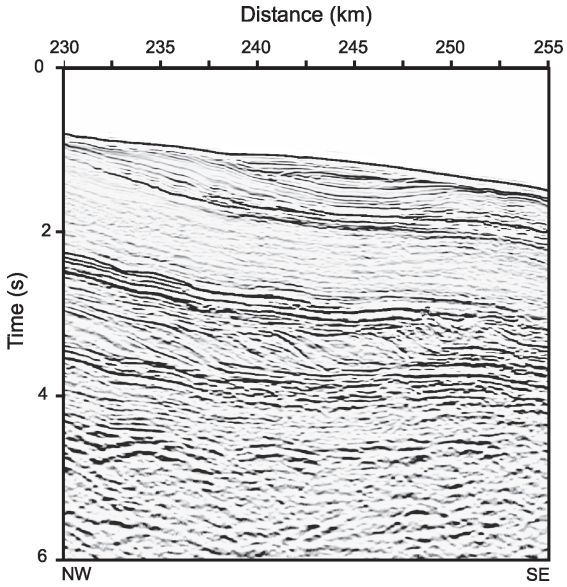

Fig. 12. Section of migrated seismic profile crossing the basalt escarpment on the northwestern flank of the Faroe–Shetland Trough (from Christie *et al*. 2004). See Figure 10 for location of this 25 km long extract. Processing includes source designature, multiple suppression and migration. Strong sigmoidal foresets are well imaged within the basalt sequence between 3 and 4s two-way travel time: these are interpreted as the palaeo-coastline in this region when the lavas were extruded. Data shown with permission of WesternGeco.

Conclusions

Use of wide-angle arrivals, whether from long offset streamers or OBS, together with a large deep-towed seismic source, allows for effective imaging of the deep structure within and beneath heterogeneous basalt flows. We have imaged the crustal evolution across the volcanic continent–ocean boundary near the Faroe Islands, including clear imaging both of the massive extrusive lava flows represented by seaward dipping reflector sequences, the layering caused by crustal intrusion in the underlying stretched continental crust, and the development of a Moho reflection which can be traced across the boundary from continental to oceanic crust. On the continental side, a similar quality of imaging has been achieved, with structure visible both within and beneath the basalts that flowed toward the Faroes–Shetland Trough.

Our future work on this excellent dataset will include close integration between the seismic reflection data and the wide-angle arrivals to enhance deep crustal and sub-basalt imaging. Control on the physical properties such as the P- and S-wave structure, the degree of anisotropy and absorption characteristics of the subsurface, which are possible by combining the long-offset streamer and the four-component OBS data, will allow us to put tighter constraints on evolutionary models of the interplay between rifting and magmatism in this classic area of a volcanic continental margin.

The authors wish to thank the Masters and crews of both the *RRS Discovery* and the *M/V Geco Topaz* for their expertise in acquiring high-quality datasets. We thank P. Sabel, J.-F. Hopperstad, A. Harber, A. Langridge and J. Bacon of WesternGeco for support during the pre-survey modelling and processing of the Q-data. We thank R England for his review and detailed comments on the manuscript. The iSIMM project is supported by Liverpool and Cambridge Universities, Schlumberger Cambridge Research, Badley Technology Limited, WesternGeco, Agip, Amerada Hess, Anardarko, BP, Conoco, Phillips, Statoil, Shell, the Natural Environment Research Council (NERC) and the Department of Trade and Industry. The OBS were provided by GeoPro GmbH. University of Cambridge contribution number ES7649.

References

Andersen, M. S. 1988. Late Cretaceous and Palaeogene extension and volcanism around the Faeroe Islands. *In*: Morton, A. C. & Parson, L. M. (eds) *Early Tertiary Volcanism and the Opening of the NE Atlantic*. Geological Society, London, Special Publications, **39**, 115–122.

Avedik, F., Hirn, A., Renard, V., Nicolich, R., Olivet, J. L. & Sachpazi, M. 1996. Single bubble marine source offers new perspectives for lithospheric exploration. *Tectonophysics*, **267**, 57–71.

Barton, A. J. & White, R. S. 1997*a*. Volcanism on the Rockall continental margin. *Journal of the Geological Society*, London, **154**, 531–536.

Barton, A. J. & White, R. S. 1997*b*. Crustal structure of the Edoras Bank continental margin and mantle thermal anomalies beneath the North Atlantic. *Journal of Geophysical Research*, **102**, 3109–3129.

Bown, J. W. & White, R. S. 1995. Effect of finite extension rate on melt generation at rifted continental margins. *Journal of Geophysical Research*, **100**, 18011–18029.

Brozena, J. M. *Kinematic GPS and Aerogeophysical Measurement: Gravity, Topography and Magnetics*. PhD thesis, University of Cambridge.

Christie, P., Langridge, A., White, R., Lunnon, Z., Roberts, A. W. & iSIMM team. 2004. iSIMM looks beneath basalt for both industry and university research. Extended abstract presented to the 5th Conference of the *Society of Petroleum Geophysicists*, *Hyderabad*, *India 15–17* January 2004.

Christie, P. A. F., Gollifer, I. & Cowper, D. 2002. Borehole seismic results from the Lopra Deepening Project. *Journal of the Conference Abstracts*, **7**, 138–139.

Cox, K. G. 1980. A model for flood basalt volcanism. *Journal of Petrology*, **21**, 629–650.

Dancer, P. N., Kenyon-Roberts, S. M., Downey, J. W., Baillie, J. M., Meadows, N. S. & Maguire, K. 2004. The Corrib Gas Field, offshore west of Ireland. *In*: Doré, A. G. & Vining, B. A. (eds) *Petroleum Geology: North-West Europe and Global Perspectives—Proceedings of the 6th Petroleum Geology Conference*. Geological Society, London, 1035–1046.

Eldholm, O. & Grue, K. 1994. North Atlantic volcanic margins: dimensions and production rates. *Journal of Geophysical Research*, **99**, 2955–2988.

Fliedner, M. M. & White, R. S. 2001. Sub-basalt imaging in the Faeroe–Shetland Basin with large-offset data. *First Break*, **19**, 247–252.

Holbrook, W. S., Larsen, H. C., Korenaga, J., Dahl-Jenson, T., Reid, I. D., Kelemen, P. B., Hopper, J. R., Kent, G. M., Lizarralde, D., Bernstein, S. & Detrick, R. S. 2001. Mantle thermal structure and active upwelling during continental breakup in the North Atlantic. *Earth and Planetary Science Letters*, **190**, 251–266.

Jones, S. M. & White, N. 2003. Shape and size of the starting Iceland plume swell. *Earth and Planetary Science Letters*, **216**, 271–282.

Kjørboe, L. 1999. Stratigraphic relationships of the Lower Tertiary of the Faeroe Basalt Plateau and the Faeroe − Shetland Basin. *In*: Fleet, A. J. & Boldy, S. A. R. (eds) *Petroleum Geology of Northwest Europe: Proceedings of the 5th Conference*. Geological Society, London, 559–572.

Korenaga, J., Holbrook, W. S., Kent, G. M., Kelemen, P. B., Detrick, R. S., Larsen, H.-C., Hopper, J. R. & Dahl-Jensen, T. 2000. Crustal structure of the southeast Greenland margin from joint refraction and reflection seismic tomography. *Journal of Geophysical Research*, **105**, 21591–21614.

Larsen, L. M., Waagstein, R., Pedersen, A. K. & Storey, M. 1999. Trans-Atlantic correlation of the Palaeogene volcanic successions in the Faeroe Islands and East Greenland. *Journal of the Geological Society*, **156**, 1081–1095.

Lunnon, Z. C., Christie, P. A. F. & White, R. S. 2003. An evaluation of peak and bubble tuning in sub-basalt seismology: modelling and results. *First Break*, **21**, 51–56.

Maresh, J., Hobbs, R. W., White, R. S. & Smallwood, J. R. 2003. Attenuation of Atlantic margin basalts using downhole VSP (extended abstract), *73rd Annual International Meeting: Society of Exploration Geophysicists, Dallas*, 1310–1313.

Morgan, J. V., Barton, P. J. & White, R. S. 1989. The Hatton Bank continental margin-III. Structure from wide-angle OBS and multichannel seismic refraction profiles. *Geophysical Journal International*, **98**, 367–384.

Naylor, P. H., Bell, B. R., Jolley, D. W., Durnall, P. & Fredsted, R. 1999. Palaeogene magmatism in the Faeroe–Shetland Basin: influences on uplift history and sedimentation. *In*: Fleet, A. J. & Boldy, S. A. R. (eds) *Petroleum Geology of Northwest Europe: Proceedings of the 5th Conference*. Gelogical Society, London, 545–558.

Richardson, K. R., Smallwood, J. R., White, R. S., Snyder, D. & Maguire, P. K. H. 1998. Crustal structure beneath the Faroe Islands and the Faroe–Iceland Ridge. *Tectonophysics*, **300**, 159–180.

Richardson, K. R., White, R. S., England, R. W. & Fruehn, J. 1999. Crustal structure east of the Faroe Islands. *Petroleum Geoscience*, **5**, 161–172.

Roest, W. R. & Srivastava, S. P. 1989. Sea-floor spreading in the Labrador Sea: a new reconstruction. *Geology*, **17**, 1000–1003.

Saunders, A. D., Fitton, J. G., Kerr, A. C., Norry, M. J. & Kent, R. W. 1997. The North Atlantic Igneous Province. In: Mahoney, J.J. & Coffin, M.F. (eds). *American Geophysical Union*, *Geophysical Monograph*, **100**, 45–93.

Smallwood, J. R. & Maresh, J. 2002. The properties, morphology and distribution of igneous sills: modelling, borehole data and 3D seismic from the Faroe-Shetland area. *In*: Jolley, D. W. & Bell, B. R. (eds) *The North Atlantic Igneous Province: Stratigraphy, Tectonic, Volcanic and Magmatic Processes*. Geological Society, London, Special Publications, **197**, 271–306.

Smallwood, J. R. & White, R. S. 1998. Crustal accretion at the Reykjanes Ridge, 61–62°N. *Journal of Geophysical Research*, **103**, 5185–5201.

Smallwood, J. R. & White, R. S. 2002. Ridge-plume interaction in the North Atlantic and its influence on continental break-up and seafloor spreading. *In*: Jolley, D. W. & Bell, B. R. (eds) *The North Atlantic Igneous Province: Stratigraphy, Tectonic, Volcanic and Magmatic Processes*. Geological Society, London, Special Publications, **197**, 15–37.

Smallwood, J. R., Staples, R. K., Richardson, K. R. & White, R. S. & FIRE Working Group 1999. Crust generated above the Iceland mantle plume: from continental rift to oceanic spreading center. *Journal of Geophysical Research*, **104**, 22885–22902.

Smith, L. K., White, R. S., Kusznir, N. J. & iSIMM Team. 2004. Structure of the Hatton Basin and adjacent continental margin. *In*: Doré, A. G. & Vining, B. A. (eds) *Petroleum Geology: North-West Europe and Global Perspectives—Proceedings of the 6th Petroleum Geology Conference*. Geological Society, London, 947–956.

Sorensen, A. B. 2003. Cenozoic basin development and stratigraphy of the Faroes area. *Petroleum Geoscience*, **9**, 189–207.

Staples, R. K., Hobbs, R. W. & White, R. S. 1999. A comparison between airguns and explosives as wide-angle seismic sources. *Geophysical Prospecting*, **47**, 313–339.

Vogt, P. R. 1971. Asthenospheric motion recorded by the ocean floor south of Iceland. *Earth and Planetary Science Letters*, **13**, 153–160.

Waagstein, R. 1988. Structure, composition and age of the Faeroe basalt plateau. *In*: Morton, A. C. & Parson, L. M. (eds) *Early Tertiary Volcanism and the Opening of the NE Atlantic*. Geological Society, London, Special Publications, **39**, 225–238.

White, N. J. & Lovell, B. 1997. Measuring the pulse of a plume with the sedimentary record. *Nature*, **387**, 888–891.

White, R. & McKenzie, D. 1989. Magmatism at rift zones: the generation of volcanic continental margins and flood basalts. *Journal of Geophysical Research*, **94**, 7685–7729.

White, R. & McKenzie, D. 1995. Mantle plumes and flood basalts. *Journal of Geophysical Research*, **100**, 17543–17585.

White, R. S. 1997. Rift-plume interaction in the North Atlantic. *Philosophical Transactions of the Royal Society, London, Series A*, **355**, 319–339.

White, R. S., McKenzie, D. & O'Nions, R. K. 1992. Oceanic crustal thickness from seismic measurements and rare earth element inversions. *Journal of Geophysical Research*, **97**, 19683–19715.

White, R. S., Fruehn, J., Richardson, K. R., Cullen, E., Kirk, W., Smallwood, J. R. & Latkiewicz, C. 1999. Faroes Large Aperture Research Experiment (FLARE): Imaging through basalts. *In*: Fleet, A. J. & Boldy, S. A. R. (eds) *Petroleum Geology of Northwest Europe: Proceedings of the 5th Conference*. Geological Society, London, 1243–1252.

White, R. S., Christie, P. A. F., Kusznir, N. J., Roberts, A., Hurst, N., Lunnon, Z., Parkin, C. J., Roberts, A. W., Smith, L. K., Spitzer, R., Surendra, A. & Tymms, V. 2002. iSIMM pushes frontiers of marine seismic acquisition. *First Break*, **20**, 782–786.

White, R. S., Smallwood, J. R., Fliedner, M. M., Boslaugh, B., Maresh, J. & Fruehn, J. 2003. Imaging and regional distribution of basalt flows in the Faroe–Shetland Basin. *Geophysical Prospecting*, **51**, 215–231.

Ziolkowski, A., Parkes, G., Hatton, L. & Haugland, T. 1982. The signature of an air-gun array – Computation from near-field measurements including interactions. *Geophysics*, **47**, 1413–1421.

Ziolkowski, A., Hanssen, P., Gatliff, R., Jakubowicz, H., Dobson, A., Hampson, G., Li, X.-Y. & Liu, E. 2003. Use of low frequencies for sub-basalt imaging. *Geophysical Prospecting*, **51**, 169–182.